ARTICLE
Journal of Cellular Biochemistry 108:693–704 (2009)

Journal of Cellular Biochemistry

Clonal Mesenchymal Stem Cells Derived From Human Bone Marrow Can Differentiate Into Hepatocyte-Like Cells in Injured Livers of SCID Mice

Xin-Rong Tao,[1,2] Wen-Lin Li,[1] Juan Su,[1] Cai-Xia Jin,[1] Xin-Min Wang,[1] Jian-Xiu Li,[1] Jun-Kai Hu,[1] Zhen-Hua Xiang,[3] Joseph T.Y. Lau,[4] and Yi-Ping Hu[1*]

[1]*Department of Cell Biology, Second Military Medical University, 800 Xiangyin Rd., Shanghai 200433, PR China*
[2]*Department of Cell Biology, Medical College, Anhui University of Science & Technology, Huainan 232001, PR China*
[3]*Department of Neural Science, Second Military Medical University, 800 Xiangyin Rd., Shanghai 200433, PR China*
[4]*Department of Molecular and Cellular Biology, Roswell Park Cancer Institute, Elm and Carlton Streets, Buffalo, New York 14263*

ABSTRACT

There is increasing evidence that human mesenchymal stem cells (hMSCs) can be a valuable, transplantable source of hepatocytes. Most of the hMSCs preparations used in these studies were likely heterogeneous cell populations, isolated by adherence to plastic surfaces or by density gradient centrifugation. Therefore, the participation of other unknown trace cell populations cannot be rigorously discounted. Here we report the isolation and establishment of a cloned human MSC line (chMSC) from human bone marrow primary culture, through which we confirmed the hepatic differentiation capability of authentic hMSCs. chMSCs expressed markers of mesenchymal cells, but not markers of hematopoietic stem cells. In vitro, chMSCs can differentiate into either mesenchymal cells or cells exhibiting hepatocyte-like phenotypes. When transplanted intrasplentically into carbon tetrachloride-injured livers of SCID mice, EGFP-tagged chMSCs engrafted into the host liver parenchyma, exhibited typical hepatocyte morphology, form a three-dimensional architecture, and differentiate into hepatocyte-like cells expressing human albumin and α-1-anti-trypsin. By confocal microscopy, ultrafine intercellular nanotubular structures were visible between adjacent transplanted and host hepatocytes. We postulate that these structures may assist in the phenotype conversion of chMSCs, possibly by exchange of cytoplasmic components between native hepatocytes and transplanted cells. Thus, a clonal pure population of hMSCs, which can be expanded in culture, may have potential as a cellular source for substitution damaged cells in hepatic injury. J. Cell. Biochem. 108: 693–704, 2009.

KEY WORDS: HUMAN MESENCHYMAL STEM CELLS; HEPATIC DIFFERENTIATION; STEM CELL TRANSPLANTATION; CELL THERAPY

Stem cells from both hepatic and extrahepatic origins have been evaluated for their potential involvement in liver repair after injury. There is much evidence that liver progenitors, and even mature hepatocytes, can repopulate the injured liver [Rhim et al., 1994; Coleman et al., 1997; Malhi et al., 2002]. Hepatocyte transplantation is a potential therapeutic approach for many liver diseases [Gupta and Chowdhury, 2002]. However, because of the paucity of hepatocytes available for grafts, and inherent dangers when mixtures of cells or uncharacterized starting material are used as donors (e.g., viral load, tumorigenesis, etc.), it is highly desirable to identify alternative cell sources that can repair the liver after injury.

Extrahepatic stem cells such as hematopoietic stem cells (HSCs) or mesenchymal stem cells (MSCs), could also generate hepatocytes in damaged livers [Lagasse et al., 2000; Aurich et al., 2007]. By using the fumarylacetoacetate hydrolase (FAH) knockout mouse model, Lagasse et al. [2000] demonstrated that mouse HSCs could give rise to hepatocytes and rescue fatal liver damage. Hepatic differentiation

Xin-Rong Tao and Wen-Lin Li contributed equally to this work.

Grant sponsor: National Natural Science Foundation of China; Grant numbers: 30470876, 30600326; Grant sponsor: Chinese National 863 Project; Grant number: 2006AA02Z474; Grant sponsor: Shanghai Key Basic Science Project; Grant number: 06DJ14001; Grant sponsor: National Basic Research Program of China; Grant numbers: 2009CB941100, 2010CB945602; Grant sponsor: NIH; Grant number: AI056082.

*Correspondence to: Yi-Ping Hu, Department of Cell Biology, Second Military Medical University, 800 Xiangyin Rd., Shanghai 200433, PR China. E-mail: yphu@smmu.edu.cn

Received 5 October 2008; Accepted 14 July 2009 • DOI 10.1002/jcb.22306 • © 2009 Wiley-Liss, Inc.
Published online 19 August 2009 in Wiley InterScience (www.interscience.wiley.com).

of human HSCs has also been demonstrated in experimentally damaged liver of SCID mice, such as by irradiation or hepatotoxicant exposure [Kakinuma et al., 2003; Kollet et al., 2003; Newsome et al., 2003; Wang et al., 2003; Sakaida et al., 2004; Yamamoto et al., 2004]. However, the utility of HSCs as a source of hepatocyte population is functionally limited by the difficulties in expanding human HSCs in culture.

MSCs are fibroblast-like, non-hematopoietic, and plastic-adherent cells, which can be isolated from various tissues [Jiang et al., 2002a,b]. MSCs exhibit the potential of differentiating into mesenchymal tissues such as adipose, cartilage, and bones [Pittenger et al., 1999]. Their capacity to differentiate into cells of other tissues, such as cardiac myocytes, neurons, and hepatocytes, has also been reported [Barbash et al., 2003; Munoz-Elias et al., 2004; Lee et al., 2004]. The hepatic differentiation potential of MSCs has drawn increasing interest, and may provide an unlimited source of cells for hepatocyte replacement therapies [Dahlke et al., 2004; Fang et al., 2004; Sato et al., 2005; Aurich et al., 2007; Chamberlain et al., 2007].

Previous reports demonstrated that human MSCs can participate in liver regeneration [Sato et al., 2005; Aurich et al., 2007]. However, the human MSCs in these studies were heterogeneous populations that were not clonally purified. Hence, contribution from trace, unknown cell types in the hepatocyte differentiation process cannot be rigorously excluded.

In the present study, we took advantage of the well-known properties of MSCs to adhere on plastic surface and to form colonies in culture to isolate and to establish cloned MSC lines from a primary culture of human bone marrow cells. These cloned MSC lines, which we term clonal human mesenchymal stem cells (chMSCs), possess the potential to give rise to either mesenchymal cells or hepatocytes under appropriate in vitro culture conditions. After transplantation into carbon tetrachloride-injured livers of SCID mice, chMSCs could engraft in the liver parenchyma. Engrafted chMSCs persisted for at least 8 weeks post-transplantation and formed three-dimensional architecture in host livers. Intercellular nanotubular connections [Rustom et al., 2004], visualized by confocal microscopy, formed between chMSC-derived hepatocytes and recipient hepatocytes. These structures may contribute to hepatocyte phenotype establishment of chMSCs, possibly by interchange of cellular components between transplanted cells and host hepatocytes [Gerdes et al., 2007].

MATERIALS AND METHODS

All cell culture reagents were purchased from Gibco BRL (Rockville, MD), and all chemicals were obtained from Sigma–Aldrich (St. Louis, MO) unless specified elsewhere.

ISOLATION AND CULTURE OF chMSCs

Bone marrow aspirates were obtained from the iliac crest of healthy donors (n = 9) after informed consent. Cells were recovered from 5 ml of heparinized BM aspirate after washing twice with phosphate-buffered saline (PBS) by centrifugation at 900*g* for 15 min at 4°C. After removing RBCs by ammonium chloride lysis, a single cell suspension, obtained by pipetting through a 19 G syringe, was plated at a density of $1 \times 10^4/cm^2$. After 24 h, non-adherent cells were removed from culture by PBS washes and subsequent medium changes every 3–4 days thereafter. The cells were maintained in low-glucose Dulbecco's Modified Eagle's Medium (DMEM) supplemented with 10% fetal bovine serum (FBS; Hyclone, UT, lot number: ALK14881), 2 mM Glutamax, 100 U/ml penicillin, and 100 μg/ml streptomycin at 37°C with 5% CO_2. Actively proliferating clones containing homogeneous fibroblastic cells were picked with sterile pipette tips under microscope and then transferred into wells of a 24-well plate, and subsequently expanded in 60-mm dishes. These fibroblastic cell populations were further purified by limiting dilution to obtain single cell-derived human MSC. Briefly, a single cell suspension, obtained after being treated with 0.05% trypsin containing 0.53 mM EDTA, was plated into the wells of 96-well plates at a density of 0.5 cells in 100 μl culture medium per well. Phase-contrast microscopy was used to identify wells containing a single cell; only those clones derived from a single cell were selected for expansion and further experimentation. These single cell-derived fibroblastic cells were named chMSCs. chMSCs were reseeded and expanded in culture dishes at a density of 50–500 cells/cm^2 as soon after reaching 60% confluence.

FLUORESCENCE-ACTIVATED CELL SORTING AND DNA PLOIDY ANALYSIS

For fluorescence-activated cell sorting (FACS) analysis, 10^6 cells from 6 and 10 passage were detached, washed with PBS, and incubated (20 min at room temperature) with fluorescein isothiocyanate (FITC)-coupled antibodies against CD3, CD34, CD45, CD90, CD44, and HLA-1; phycoerythrin (PE)-coupled antibodies against CD13, CD14, CD29, CD133, CXCR4, and HLA-DR, or corresponding control antibodies (Santa Cruz, CA). Cells were analyzed by using a FACS-Calibur (Becton Dickinson) with CellQuest software. DNA content per cell was determined by FACS analysis after staining the 10 and 16 passage chMSCs with propidium iodide. Peripheral blood mononuclear cells from a healthy human were used as a control.

RT-PCR ANALYSIS

Total RNA was extracted from cultured cells with Trizol reagent (Sangon, Shanghai, China). RNA concentration was calculated based on UV absorption. Reverse transcription was performed with 2 μg RNA, random hexamers (TaKaRa, Dalian), and M-MLV reverse transcriptase (Promega, WI) according to the manufacturer's recommended protocol. The first-strand cDNA product was subjected to PCR analysis using the gene-specific primer pairs listed in Table I. The PCR conditions were an initial denaturation at 95°C for 5 min. This was followed by 36 cycles of 94°C for 30 s, annealing temperature for 60 s depending on the primer pair, and 72°C for 60 s. The final cycle was followed by 72°C for 10 min. RT-PCR products and pUC Mix DNA marker (MBI, Fermentas) were applied to 1.5% agarose gel for electrophoresis.

IN VITRO DIFFERENTIATION

chMSCs at passage 7 to 13 were evaluated for their differentiation abilities. To induce osteogenesis, chMSCs were plated at a density of 5×10^3 cells/cm^2 in osteogenic medium containing DMEM-HG

TABLE I. The Primers Used for RT-PCR Analysis

Genes	Primer sequence	PCR size (bp)
CD49a	5′-CTGCTACTGCTTCTTCTGGAG-3′ 5′-CCACCTGATGGAATACGTTGTGC-3′	550
c-Kit	5′-CGTTGACTATCAGTTCAGCGAG-3′ 5′-CTGGGAATGTGTAAGTGCCTCC-3′	360
c-Met	5′-GGGTCGCTTCATGCAGGTTGTGGT-3′ 5′-ATGGTCAGCCTTGTCCCTCCTTCA-3′	372
Oct4A	5′-CGTGAAGCTGGAGAAGGAGAAGCTG-3′ 5′-CAAGGGCCGCAGCTTACACATGTTC-3′	247
α-SMA	5′-GCTCACGGAGGCACCCCTGAA-3′ 5′-CTGATAGGACATTGTTAGCAT-3′	590
SDF-1α	5′-ATGAACGCCAAGGTCGTGGTCG-3′ 5′-TGTTGTTGTTCTTCAGCCG-3′	202
Osteopontin	5′-CTAGGCATCACCTGTGCCATACC-3′ 5′-CAGTGACCAGTTCATCAGATTCATC-3′	373
Aggrecan	5′-TGA GGAGGGCTGGAACAAGTACC-3′ 5′-GGAGGTGGTAATTGCAGGGAACA-3′	350
PPARγ2	5′-GCTGTTATGGGTGAAACTCTG-3′ 5′-ATAAGGTGGAGATGCAGGCTC-3′	351
Alb	5′-CCTTTGGCACAATGAAGTGGGTAACC-3′ 5′-CAGCAGTCAGCCATTTCACCATAGG-3′	355
AFP	5′-ATTCAGACTGCTGCAGCCAA-3′ 5′-GTGCTCATGTACATGGGCCA-3′	476
G6P	5′-GGCACAGCAGGTGTATACTA-3′ 5′-AGAGGACCACCTGAGCTGAC-3′	1101
TAT	5′-TGAGCAGTCTGTCCACTGCCT-3′ 5′-CATGTGAATGAGGAGGATCTGAG-3′	358
CYP1B1	5′-GAGAACGTACCGGCCACTATCACT-3′ 5′-GTTAGGCCACTTCACTGGGTCATGAT-3′	357
TDO	5′-ATACAGAGCACTTCAGGGAGC-3′ 5′-TGGTTGGGTTCATCTTCGGTATC-3′	299
HNF4α	5′-CCAAGTACATCCCAGCTTTC-3′ 5′-TTGGCATCTGGGTCAAAG-3′	295
β-actin	5′-GCACTCTTCCAGCCTTCCTTCC-3′ 5′-TCACCTTCACCGTTCCAGTTTTT-3′	516

SDF-1α, stromal cell-derived factor-1α; *c-kit*, Stem Cell Factor, SCF receptor; *c-Met*, a specific receptor for HGF; *α-SMA*, alpha-smooth muscle actin; *AAT*, α-anti-trypsin; *Alb*, albumin; *AFP*, α-fetoprotein; *TAT*, tyrosine-aminotransferase; *G6P*, glucose-6-phosphatase; *HNF4α*, hepatocyte nuclear factor-4α; *TDO*, tryptophan 2,3-dioxygenase; *CYP1B1*, cytochrome P450 1B1; β-actin, beta-actin.

supplemented with 10 mM β-glycerophosphate, 10^{-7} M dexamethasone, 0.2 mM ascorbic acid. chMSCs were fed every 3–4 days. After culture for 2 weeks, the cells were stained with Alizarin red S to reveal the calcium deposition. The expression of type I collagen, and osteopontin was analyzed by immunocytochemistry and RT-PCR.

For chondrocyte differentiation, a micromass culture system was used. Approximately 2.5×10^5 cells were pelleted into micromasses by centrifugation at 2,000 rpm for 10 min. The pellets were cultured in chondrogenic medium containing serum-free high-glucose DMEM supplemented with 10 ng/ml TGF-β1 (Peprotech, London), 10^{-7} M dexamethasone, 1 mM pyruvate, and ITS + Premix. Dilutions of ITS + Premix contain final concentrations of 5 μg/ml insulin from bovine pancreas, 5 μg/ml human transferrin (substantially iron free), 5 ng/ml sodium selenite, 1.25 mg/ml bovine serum albumin, and 5.35 mg/ml linoleic acid. After 21 days in culture, the pellets were fixed in 4% paraformaldehyde and sectioned into cryostat sections (5 μm in thickness). Sulfated glycosaminoglycan was visualized with 1% toluidine blue staining. Deposition of cartilage-specific type II collagen was revealed with anti-type II collagen monoclonal antibody (Santa Cruz). RT-PCR was used to analyze the expression of chondrogenesis-specific gene aggrecan.

For adipogenic differentiation, high-glucose DMEM supplemented with 5% FBS, 1 μM dexamethasone, 0.5 mM isobutylmethylxanthine, 0.2 mM indomethacin, and 10 μg/ml Insulin was used as adipogenic induction medium (AIM). High-glucose DMEM supplemented with 5% FBS and 10 μg/ml Insulin was used as adipogenic maintaining medium (AMM). Cells were plated at density of 2×10^4 cells/cm^2. Two-day post-confluence, cells were incubated 3 days in AIM followed by 3 days in AMM and then switched to AIM again. After the third cycle, cells were fed AMM for up to 21 days. The adipogenic cultures were fixed in 10% formalin for 10 min and stained with fresh Oil Red-O solution. RT-PCR was used to analyze expression of adiogenesis-specific gene peroxisome proliferator activating receptor-γ2 (PPARγ2).

For chMSC differentiate into hepatocyte-like cells, the method described by Lee et al. [2004] was used with minor modifications. chMSCs were treated in pre-induction medium, consisting of Iscoves modified Dulbecco medium (IMDM) supplemented with 2% FBS, 20 ng/ml epidermal growth factor (EGF), and 10 ng/ml fibroblast growth factor-4 (FGF-4; Peprotech) for 2 days prior to induction by a 2-step protocol. Differentiation was induced by treating chMSCs with step-1 differentiation medium consisting of IMDM supplemented with 2% FBS, 10 ng/ml FGF-4, 20 ng/ml human recombinant hepatocyte growth factor (HGF), and 4.7 μg/ml linoleic acid for 7 days, followed by treatment with step-2 maturation medium consisting of IMDM supplemented with 2% FBS, 10 ng/ml FGF-4, 20 ng/ml oncostatin M (OSM), 1 μM dexamethasone, and 50 μg/ml ITS + Premix. Thereafter, medium changes were performed twice weekly up to 21 days. A parallel differentiation of chMSCs was also performed except without FGF-4 in the induction medium and without OSM in step-2. Liver-associated genes listed in Table I were assessed by RT-PCR. Human albumin (Dako, Denmark) and human α-1-anti-trypsin (AAT; Dako) were analyzed by immunofluorescence. Periodic Acid-Schiff (PAS) assay was used to visualize glycogen.

TRANSDUCTION chMSCs WITH RETROVIRAL VECTOR pLNCG-C1

Retrovirus-rich DMEM media harvested from the late exponential phase PT67 packaging line, stably transfected with pLNCG C1 retroviral vector [Dirks and Miller, 2001], was sterilized through 0.45 μm filters (Millipore, Molsheim, France). The filtrate containing 4 μg/ml polybrene was added to a 40–60% confluent culture of chMSCs. After 12 h incubation, the viral supernatant was removed and then fresh complete medium was added. chMSCs were infected for two more times by following the above procedure and then subjected to selection in complete medium containing 500 μg/ml G418 for 2 weeks. After G418 selection, chMSC with homogenous EGFP expression was obtained and used in transplantation studies.

MICE TREATMENT AND chMSCs TRANSPLANTATION

SCID mice (n = 15, 4-week-old) were purchased from the Animal Breeding Center of Shanghai Institutes for Biological Sciences and kept under specific pathogen free (SPF) conditions. All animal procedures were carried out in accordance with the institutional guidelines. Acute liver damage was induced by intraperitoneal

injection of carbon tetrachloride, diluted as a 20% solution in olive oil, at a dose of 2 ml/kg body weight [Suzuki et al., 2002]. EGFP-positive chMSCs ($\sim 1 \times 10^6$ cells suspended in 200 μl of sterile PBS) were surgically injected into the spleens of recipient SCID mice (n = 12) 24 h after carbon tetrachloride administration. The mice (n = 3) in the sham control were injected with the same volume of PBS. Mice were killed at 2 (n = 4), 5 (n = 4), and 8 (n = 4) weeks post-transplantation and perfused transcardially with cold PBS followed by phosphate buffer containing 4% paraformaldehyde. Perfused livers were immersed in the same fixative at 4°C overnight and then in PBS containing 30% sucrose at 4°C overnight. Ten-micrometer-thick sections were prepared by using a cryostat and were observed under fluorescent microscopy (Nikon TE-2000U, Japan) or confocal microscopy (Leica TCS-SPII, Germany). 1×10^7 cells were transplanted subcutaneously into SCID mice (n = 3) to assess the tumor formation.

HISTOLOGICAL ANALYSIS OF THE TRANSPLANTED CELLS AND FLUORESCENT IN SITU HYBRIDIZATION (FISH)

Mouse livers were harvested at 2, 5, and 8 weeks after transplantation and fixed as described above. The contribution of EGFP-positive cells in the regenerating liver was determined using the cryostat sections of left lobes. The percentage of EGFP-expressing cells was calculated from the number of pixels in each visual field of liver cryostat sections compared with the number of pixels of EGFP-positive fields using PHOTOSHOP 6.0 (Adobe Systems) as described [Strick-Marchand et al., 2004]. A mean value for every mouse was obtained by random selection of 10 visual fields at 40×. EGFP-positive cell in clusters were counted manually in liver cryostat sections at 2 weeks post-transplantation. Results are expressed as mean ± SD. The difference between the percentage of cell participation at 2, 5, and 8 weeks post-transplantation was assessed using the ANOVA test.

For immunohistology, free-floating liver cryostat sections (10 μm in thickness) were incubated with polyclonal rabbit anti-human albumin (Alb) antibody (1:500, Dako) and polyclonal rabbit anti-human α-1-anti-trypsin (AAT) antibody (1:400, Dako), rabbit anti-goat IgG with Alexa Fluo 555 (1:250, Molecular Probes, OR) was used as secondary antibodies for 16 h at 4°C, and then stained with Alexa Fluo 555 conjugated goat anti-rabbit IgG (1:250, Molecular Probes). 4′,6′-diamidino-2-phenylindole (DAPI) (Molecular Probes) was used to stain nuclei. Polyclonal affinity purified goat anti-mouse albumin antibody (1:500, Bethyl Laboratories), which is specific to the mouse albumin and does not recognize the human albumin [vonMach et al., 2004], were also used. The same reactions without primary antibody incubation were used as negative controls.

Paraffin-embedded slides were hybridized by mouse or human chromosome-specific pan-centromeric probes (1697-MCy3-01, 1695-F-01; Cambio, Cambridge, UK) according to the STARFISH manufacturer's protocol. Briefly, 5 μm slides were dewaxed, passed through 70%, 90%, and 100% ethanol for 2 min, transferred to acetone for 10 min, and then air-dried. The slides were incubate for 1 h at 37°C in 2× saline sodium citrate (SSC) + RNase (100 μg/ml), washed with 2× SSC for 5 min, and digested with proteinase K (200 μg/ml) for 40 min at 37°C and washed in 2× SSC for 5 min. Then, slides were immersed in 0.1 M HCl for 5 min, washed with 2× SSC, dehydrated through ethanol series, and then air-dried. Sections were heated to 70°C for 2 min, and then placed in ice-cold 70% ethanol for 2 min. Serial ethanol dehydration was performed again. The samples were hybridized with the mixture of probe for 8 min at 78°C and then incubated overnight at 37°C. The next day, after washing, slides were mounted in an anti-fade containing DAPI 100 ng/ml.

RESULTS

ISOLATION, CULTURE, AND CHARACTERIZATION OF CLONAL HUMAN MESENCHYMAL STEM CELLS (chMSCs)

Single adherent cell-derived clones were harvested from primary cultures of human bone marrow cells. Thirteen primary colonies were recovered from the original seeding of 4×10^6 bone marrow mononuclear cells onto five 10-cm dishes (Falcon, BD Biosciences). Figure 1A1–A3 shows phase contrast views of the primary culture and the growth of a fibroblast-like colony at 2, 4, and 6 days, respectively, after plating. Three of the 13 primary colonies were recovered for clonal purification by limit dilution as described in Materials and Methods Section. Figure 1B1–B3 shows the growth of clone chMSC-3.1 on days 1, 5, and 8 days, respectively, after deposition as a single cell in a well of a 96-well microtiter plate. These three clones were subjected to continuous cultures. All three clones exhibited homogenous fibroblastic morphology and vigorous growth characteristics (data not shown). The homogeneous morphology of chMSC-3.1 at passage 12, 2 and 6 days after plating, is illustrated in Figure 1C1 and C2, respectively. Clone chMSC-3.1 was used for further analysis, and will be called simply as chMSCs in this report.

chMSCs retained homogeneous fibroblastic morphology and vigorous growth even after more than 16 passage and repeated cryopreservation. chMSCs had normal diploid DNA content, as visualized by FACS analysis of propidium iodide staining of chMSC-3.1 at passage 10 and at passage 16 (Fig. 1D2 and D3, respectively), and comparison to mononuclear cells from peripheral blood of normal humans as control (Fig. 1D1). The DNA content values of [G2 + M]-phase subpopulations were precisely twice the DNA content values of G1-phase subpopulations, from which we can calculate the relative percentages of cells in the G1 (2C DNA content), S (between 2C and 4C), and G2/M (4C DNA content). For chMSC-3.1, the distribution of [G1], [S], and [G2 + M] phases in the cell cycle was 83.21%, 9.6%, and 7.19%, respectively, at passage 10; and 80.61%, 13.56%, and 5.82%, respectively at passage 16. After transplanted subcutaneously into nude mice (n = 3), chMSC-3.1 at passage 16 did not develop any visible neoplasma after 3 months of observation.

chMSCs express the conventional MSC markers as demonstrated in Figure 2. Panel A shows the results of FACS analysis for cell surface markers. Essentially 100% of the cells in the chMSC culture expressed mesenchymal cell-specific markers CD13 (99.11%), CD29 (99.87%), CD44 (99.98%), and CD90 (99.75%). chMSCs was negative for the hematopoietic cell-specific markers CD3, CD14, CD34, and CD45, which is well in agreement with the antigen expression

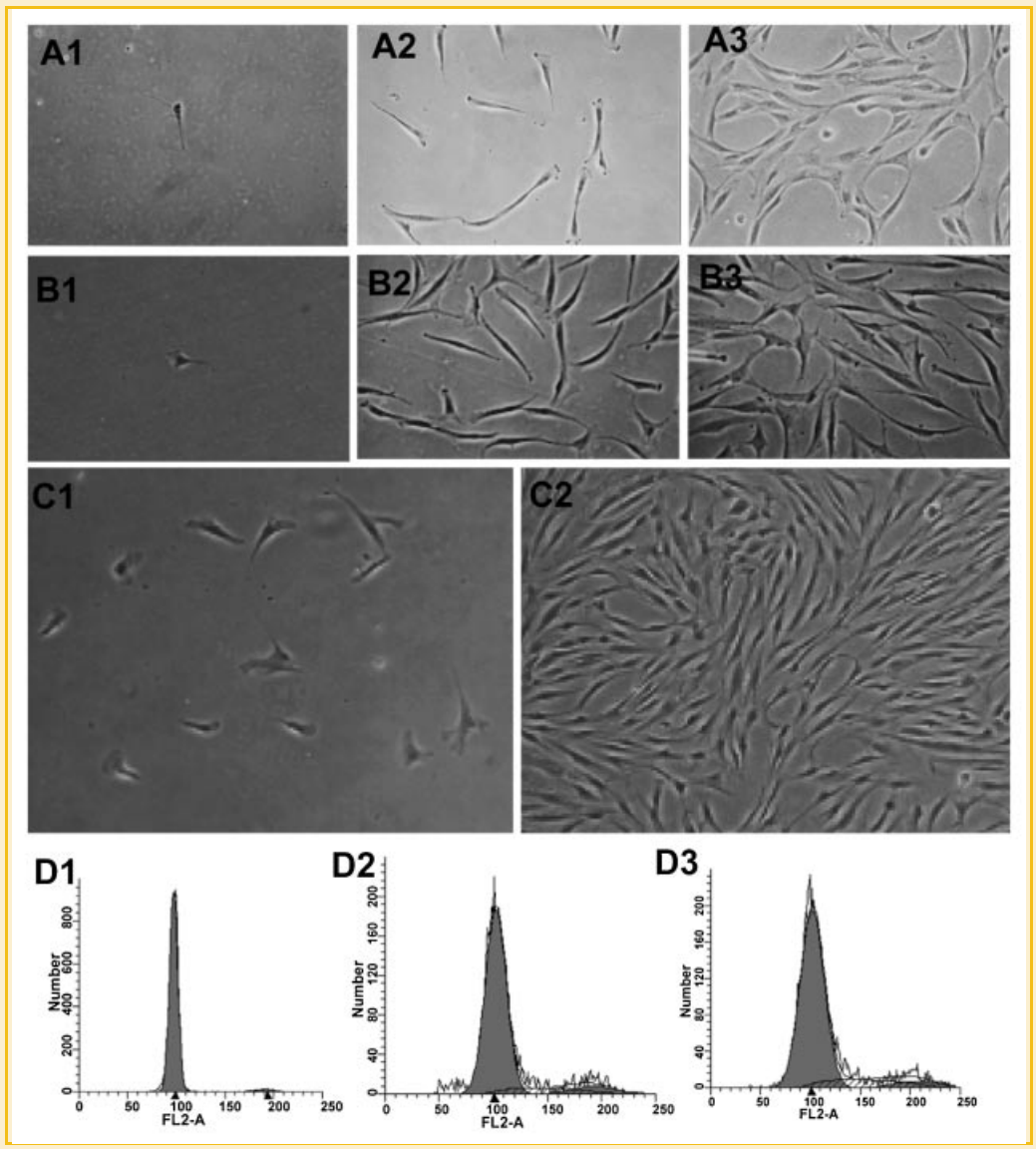

Fig. 1. Establishment of chMSCs and DNA poidy analysis. Phase-contrast images show the growth of adherent colonies arising from primary cultures of human bone marrow mononuclear cells. A1–3: Are views of the original bone marrow primary culture at 2, 4, and 6 days, respectively, after plating. Colonies arising from the primary plating were clonally purified by limit dilution. B1–3: Document clonal purification by limit dilution of clone chMSC-3.1, at 1, 5, and 8 days, respectively, after plating as a single cell. Panel C1 and C2 represent the chMSC-3.1 of passage 12 recovered from freezed stocks after 2 days and 6 days, respectively. DNA content of chMSC-3.1 was determined by FACS analysis at passage 10 (D2) and at passage 16 (D3). Mononuclear cells from normal human peripheral blood were used as control (D1). Magnification: 100×.

pattern of classical human MSCs [Pittenger et al., 1999]. chMSCs also expressed HLA-1 (98.21%), but not CD133, CXCR4, and HLA-DR. RT-PCR analysis (Fig. 2B) showed that chMSCs were positive for *SDF-1α*, alpha-smooth muscle actin (*α-SMA*), *CD49a*, and *c-Met*, but negative for *c-Kit* and *AFP* (Fig. 2B). Pluripotent stem cell marker octamer-binding transcription factor 4A (*OCT-4A*) was detected in all cultures examined (Fig. 2B).

Upon culturing in osteogenic induction medium for 2 weeks, chMSCs develop into osteogenic cells expressing alkaline phosphatase, type I collagen, and *osteopontin*. Alizarin red S staining demonstrated the calcium mineral deposition in the extracellular matrix (Fig. 3A). Under chondrogenic induction conditions for 3 weeks, chMSCs gave rise to chondrocytes with abundant glycosaminoglycan accumulation as revealed by strong toluidine blue staining (Fig. 3B). In addition, treated cells expressed type II collagen and *aggrecan* (Fig. 3B). Upon adipogenic induction, chMSC differentiation is accompanied by the formation of intracellular microdroplets, which stained positive for Oil Red O (Fig. 3C). *PPARγ2*, undetectable in untreated cells, was also induced after adipogenic induction (Fig. 3C). Above results suggested that chMSCs retained the ability to differentiate into multiple mesenchymal lineages in vitro.

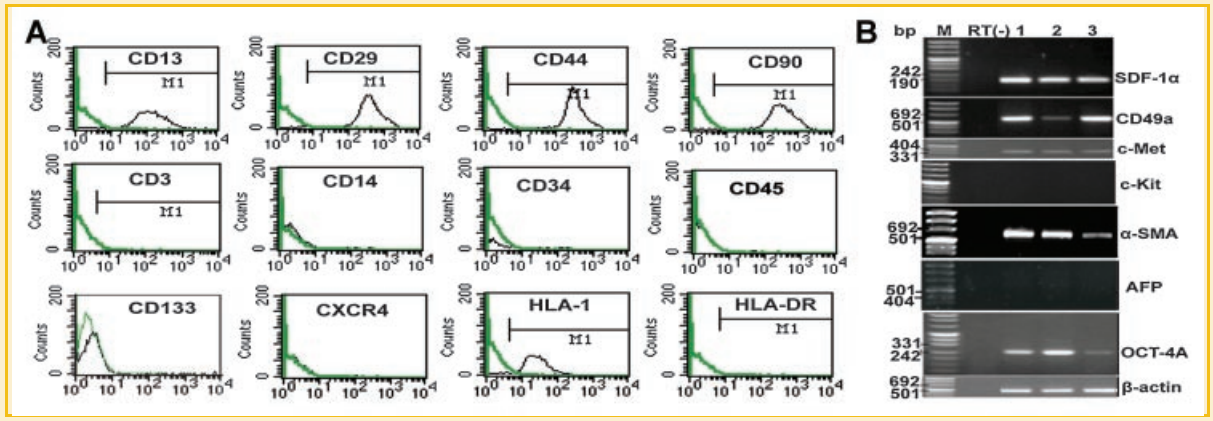

Fig. 2. chMSCs express multipotential mesenchymal stem cell markers. By FACS analysis, chMSCs expressed CD13 (99.11%), CD29 (99.87%), CD44 (99.98%), CD90 (99.75%), and HLA-1 (98.21%), but not CD3, CD14, CD34, CD45, CD133, CXCR4, and HLA-DR (A). Results from the corresponding negative isotype-matched control antibody (green lines) are also shown. Panel B: shows RT-PCR analysis of chMSCs for the indicated genes. M: pUC Mix marker; −RT: no reverse transcriptase control; lanes 1, 2, and 3: passage 6, 9, and 11 of chMSCs. Equal cDNA loading was verified by β-actin expression.

chMSCs DIFFERENTIATE INTO HEPATOCYTE-LIKE CELLS AFTER IN VITRO INDUCTION

Then the hepatocyte differentiation of chMSCs was tested in vitro. When chMSCs were subjected to induction conditions for 3 weeks, cells broadened gradually from their original spindly fibroblastic morphology (Fig. 4A), and acquired a polygonal, hepatocyte-like morphology by 21 days after initiation of induction (Fig. 4B). PAS staining revealed abundant glycogen deposition throughout the cytoplasm (Fig. 4D) which was not present in the uninduced chMSC (Fig. 4C). Differentiated cells were also positive for albumin and α1-anti-trypsin revealed by immunostaining (Fig. 4F,H), both of which were not present in the uninduced chMSCs (Fig. 4E,G). RT-PCR analysis confirmed the induction of *albumin* and *α1-anti-trypsin* mRNAs, as well as other hepatocyte functional genes *tryptophan 2,3-dioxygenase*, *glucose-6-phosphatase*, and *tyrosine aminotransferase*, none of which was present in the uninduced chMSCs. FGF-4 appeared to be essential for the establishment of the hepatic phenotype from chMSCs. In its absence, none of the surveyed hepatic mRNA markers were detected (Fig. 4I). However, complete induction into functional hepatocyte appears to require both FGF-4 and OSM (Fig. 4I). In the absence of OSM, only the early hepatocyte markers (such as *albumin* and *G6P*) were expressed but not the late marker *TAT*. *HNF4α* was only expressed in trace levels in the absence of OSM (Fig. 4I).

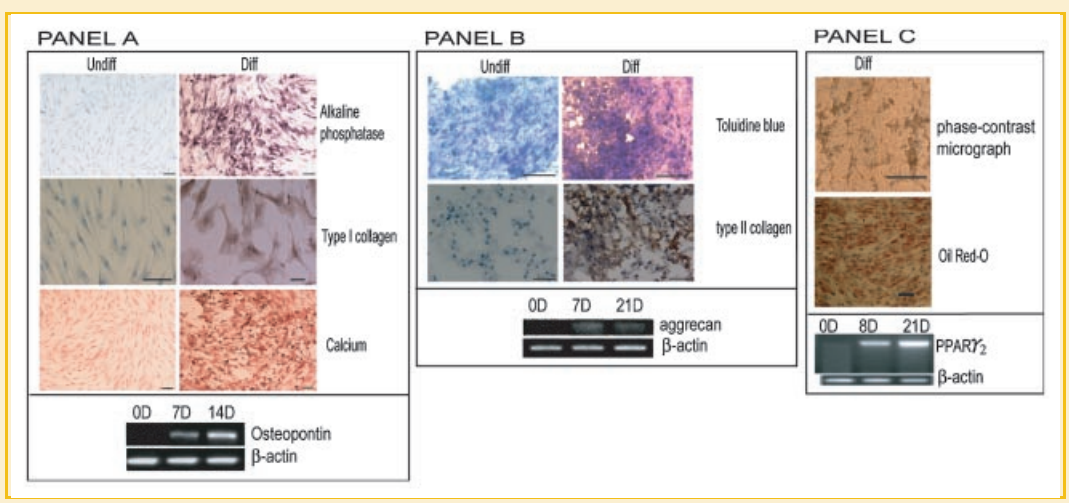

Fig. 3. chMSCs can differentiate into multiple mesenchymal lineages in vitro. chMSCs were induced to develop into osteogenic, chondrogenic, and adipogenic lineages (A, B, and C, respectively). Panel A shows the analysis for osteogenic parameters, alkaline phosphatase, type I collagen, calcium deposition, and *osteopontin* mRNA in undifferentiated (Undiff) cultures, and induction cultures for osteogenic differentiation (Diff). Panel B shows the analysis for chrondrogenic parameters, toluidine blue staining for glycosaminoglycans, type II collagen, and *aggrecan* mRNA in undifferentiated (Undiff) cells and induced cells for chrondrogenic differentiation (Diff). Panel C shows the analysis for adipogenic parameters, the formation of lipid microdroplets and Oil Red O staining, and expression of *PPARγ2* mRNA. (Scale bar: 100 μm.)

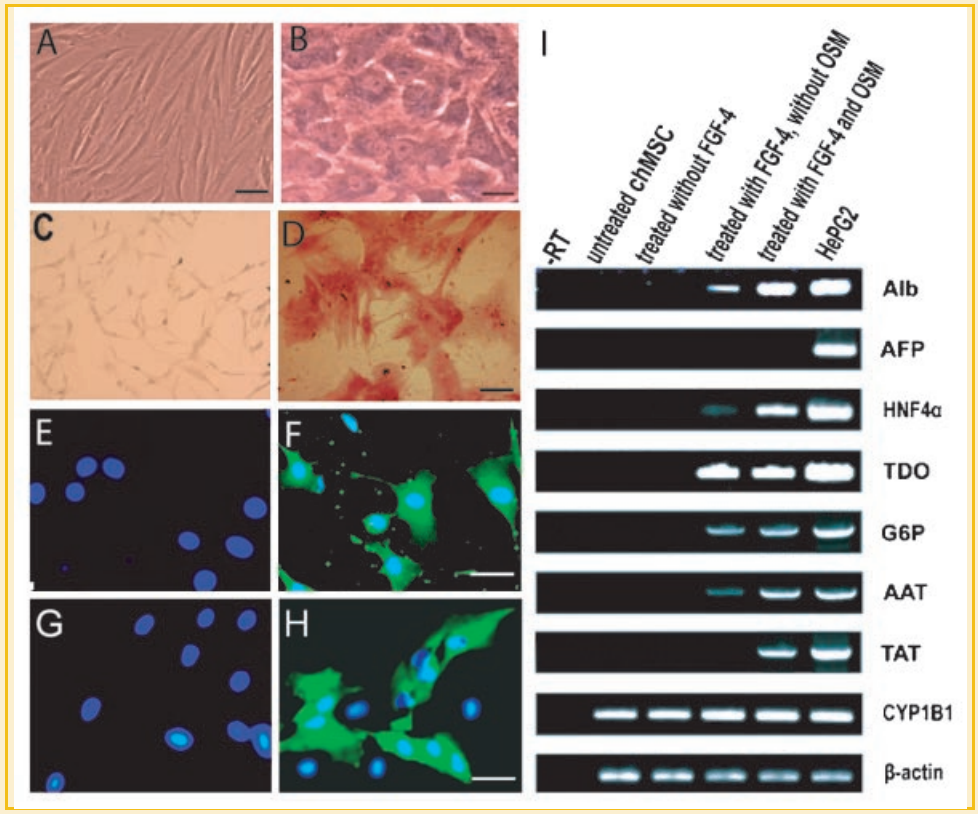

Fig. 4. chMSCs differentiate into hepatocyte-like cell in vitro. Under hepatic induction, the fibroblastic morphology of MSCs was lost and cells developed a polygonal and broadened morphology (compare A with B). PAS staining revealed abundant glycogen throughout cytoplasm in treated cells (compare C with D). Immunofluorescence analysis showed that chMSCs acquired a hepatocyte phenotype expressing albumin and AAT after induction (F,H) while untreated chMSCs were negative for albumin and AAT (E,G). Nuclei were counterstained with DAPI (scale bar: 50 μm). Panel I shows the results of RT-PCR analysis of the mRNA for *Alb*, *AFP*, *HNF4α*, *TDO*, *G6P*, *ATT*, *TAT*, *CYP1B1*, and *β-actin*. mRNA from chMSCs not treated with reverse transcriptase were performed to exclude DNA contamination (−RT). HepG2 cells as a positive control.

ENGRAFTMENT, PROLIFERATION, AND HEPATIC DIFFERENTIATION OF chMSCs IN CARBON TETRACHLORIDE-INJURED LIVERS OF SCID MICE

In order to assess the ability of chMSCs to engraft and to differentiate within the microenvironment of the injured liver in vivo, we prepared recipient animals by using the carbon tetrachloride protocol to elicit acute liver injury. chMSCs were tagged with EGFP by retroviral transduction as described in Material and Methods Section, and the tagged chMSCs uniformly expressed EGFP (Fig. 5A1 and A2). The recipient livers were harvested at 2, 5, and 8 weeks post-transplantation of the tagged chMSCs. EGFP-positive cells were completely absent when tagged chMSCs were introduced into animals without CCl_4 treatment (Fig. 5B0). This observation indicates no engraftment and repopulation of transplanted chMSCs in normal and healthy liver, consistent with published literature [Petersen et al., 1999; Lagasse et al., 2000; Kakinuma et al., 2003; Sato et al., 2005]. At 2 weeks post-transplantation (Fig. 5B1–B3), the cells derived from the transplanted chMSCs, visualized as EGFP-positive cells, had integrated into the recipient liver parenchyma. Almost all of the transplanted chMSCs converted into hepatocyte-like cells post-transplantation, which are broadened, flattened morphology with large round nuclei. EGFP-positive cells were predominantly mononucleated, and some binucleated cells (9.4% in total GFP-positive cells) were visible (arrow, Fig. 5B2). EGFP-positive cells were structurally indistinguishable from the host hepatocytes, which do not express EGFP. There was no significant difference in the engraftment efficiency of transplanted chMSCs in damaged livers between 2, 5, and 8 weeks post-transplantation ($0.22 \pm 0.08\%$, $0.21 \pm 0.08\%$, and $0.23 \pm 0.08\%$, respectively; $P > 0.05$). Representative cryostat liver sections of recipient animals at 5 and 8 weeks after transplantation are shown as Figure 5, panels C and D, respectively, with arrowheads pointing to examples of EGFP-positive cell clusters. All the EGFP-positive cells (Fig. 5G1) stained positively for human albumin (Fig. 5G2 and G3), and some, but not all of the EGFP-positive cells also reacted positively for human α1-anti-trypsin (AAT) (Fig. 5J1–J3).

EGFP expression in hepatocyte-like cells could have arisen either due to conversion of the chMSCs into hepatocytes within the host liver microenvironment, or due to cell fusion events between transplanted cells with host murine hepatocytes. To estimate the prevalence of the cell fusion mechanism, we capitalized on the property of the transplanted cells, which are human in origin that do not express mouse albumin, while only host hepatocytes expressed mouse albumin. Fusion cells, on the other hand, should be both EGFP-positive and mouse albumin positive. Immunostaining using the mouse albumin-specific antibody that did not cross-react with human hepatocytes (Fig. 6A1 and A2) can detect the fusion cells

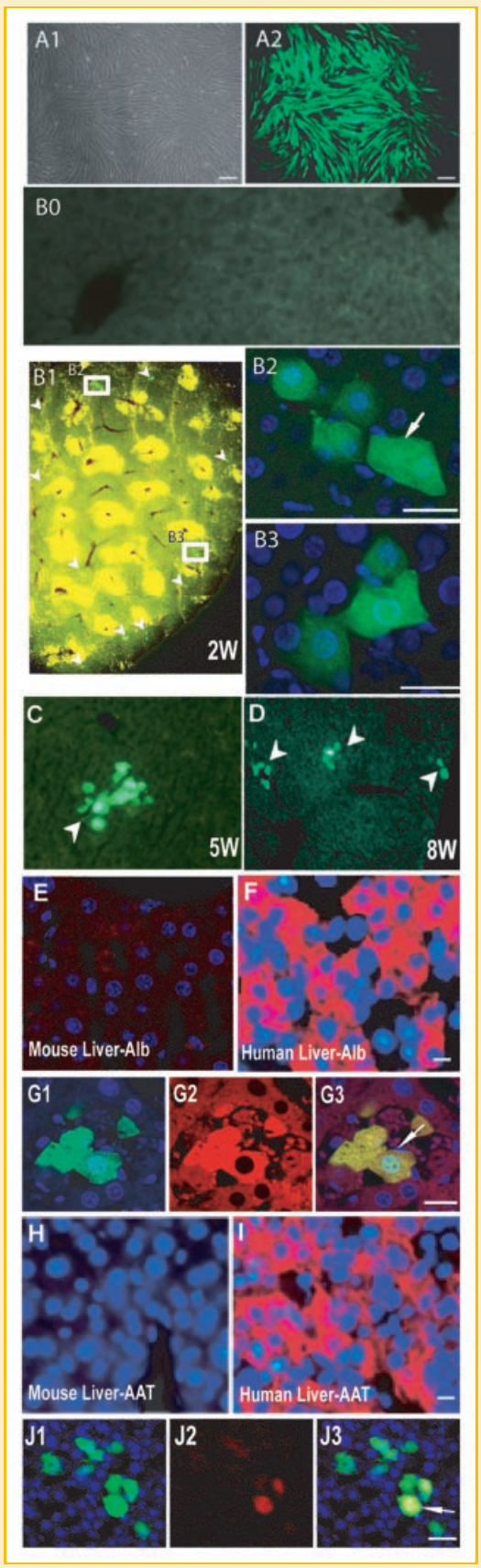

[vonMach et al., 2004]. Twenty random visual fields per recipient SCID mice (n = 12) were used to estimate the frequency of cell fusion (e.g., those EGFP-positive cells that also expressed mouse albumin). The vast majority of the EGFP-positive hepatocytes expressed human albumin, but not mouse albumin. The representative immunostaining sections were showed in Figure 6B1–B3. Arrowhead in Figure 6B3 indicated the fusion cells positive to both EGFP and mouse albumin. Based on this, we calculate the prevalence of cell fusion between donor cells and murine host cells to be minor (5.4%), and therefore the majority of the EGFP-positive hepatocyte-like cells have arisen by conversion of the chMSC donor cells. The infrequency of cell fusion events was confirmed by FISH analysis. We use mouse and human chromosome-specific pan-centromeric probes to identify the mouse and human cells in recipient mouse liver sections, respectively. Human liver cell nuclei were positively stained with human-specific probes (green: FITC; Fig. 6C1) while mouse liver cells were positively stained with mouse-specific probes (red: Cy3; Fig. 6C2). The majority of human cell nuclei in recipient mouse livers did not have mouse chromosomes (Fig. 6D1–D3).

Two weeks after transplantation, most of the chMSC-derived cells existed in the host liver as tight cell clusters (Fig. 7A). Based on a random survey of 370 EGFP-positive cells in host livers, only 21.6% of the EGFP-positive cells were present as single cells, with the majority (79.4%) existing as clusters of 2 or more EGFP-positive (Fig. 7B). These clusters exists in three-dimensional structures in the liver (Fig. 7C1 and C2). Since the survey was conducted using two-dimensional tissue sections where underlying and overlying cells cannot be seen, the actual distribution of EGFP-positive cells in multicellular clusters may be higher than indicated. Because chMSCs were transplanted as a single cell suspension, these results strongly suggest that the transplanted cells may have divided one or more times in the host liver within 2 weeks after transplantation. Confocal microscopy also revealed the presence of nanotubular-like and microvesicular-like structures linking the EGFP-expressing cells with adjacent host hepatocytes (Fig. 7D–G, red and yellow arrows, respectively). These structures are positive for EGFP, suggesting their origination from the transplanted cells. In a few instances, an EGFP signal was observed in the cell membrane and part of the cytoplasm of the host mouse hepatocytes, which were

Fig. 5. chMSCs engrafted to SCID mouse livers and differentiated into human hepatocyte-like cells. A phase contrast view of EGFP-labeled chMSCs and the corresponding fluorescent view were showed (A1, A2). EGFP-positive cells were completely absent in the SCID mouse liver without CCl4 treatment before chMSC transplantation (B0), while EGFP-positive cells were detected in the cryostat sections of CCl4-injured liver 2-week post-transplantation (B1). B2 and B3 are confocal fluorescent micrograph views of the outlined areas in B1. Arrow in B2 points to an occasional binucleated EGFP-positive cell. C and D are low magnification fluorescent views of recipient mice livers 5 and 8 weeks after EGFP-chMSC transplantation, respectively, with arrowheads pointing to some EGFP-positive cell clusters. Immunohistochemical analysis revealed that EGFP-positive cells (G1,J1) expressed human albumin (red signal; G2) and human AAT (red signal; J2). Arrowheads indicate all the EGFP-positive cells stained positively for human albumin (G3), and some, but not all of cells also reacted positively for human AAT (J3). SCID mouse and human liver sections stained with human albumin and AAT, respectively, were used as negative and positive controls. E–F and H–I. The nuclei were counterstained with DAPI. (Scale bar: A1 and A2, 100 μm; B2, B3, E–J, 20 μm.)

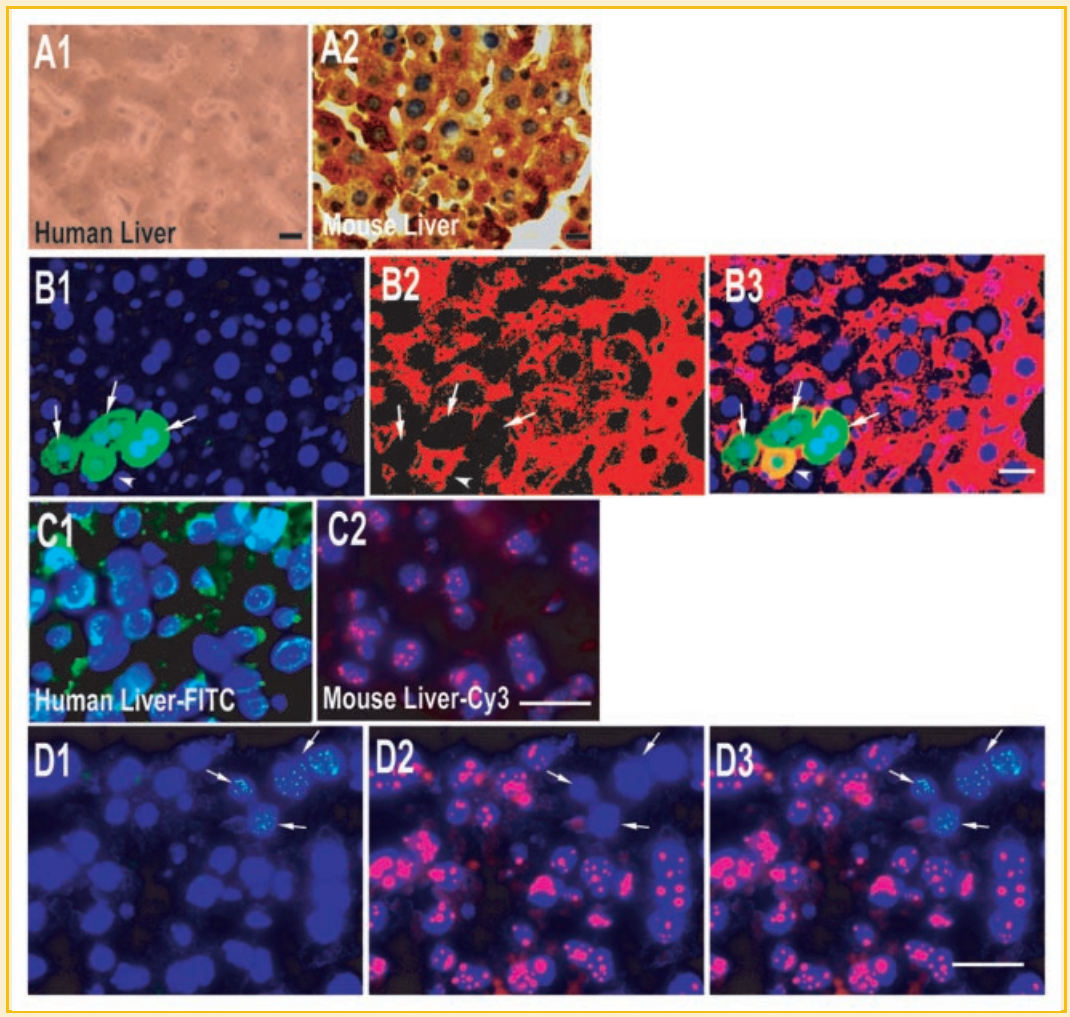

Fig. 6. chMSCs could differentiate into human hepatocytes without cell fusion with host hepatocytes in vivo. Immunohistochemistry analysis revealed that sections of human liver were not stained with antibodies specific against mouse albumin (A1) while SCID mouse liver were stained positively (A2). B1–B3: A representative cryosections of transplanted SCID mouse liver immunostained by using antibodies specific for mouse albumin. Majority of EGFP-expressing cells did not express mouse albumin (arrows), but few EGFP-expressing cells were also observed expressing mouse Alb (arrowhead). The specification of the FISH probes were confirmed by the hybridization using human liver (C1) and mouse liver section (C2). The representative FISH images of recipient mouse livers were shown in D1–D3. Green fluorescent dots for human centromeres were detected within the nuclei (arrows in D1) while red fluorescent dots for mouse centromeres were not found (arrows in D2). D3 was the overlapping of D1 and D2. The nuclei were counterstained with DAPI. (Scale bar: 20 μm.)

otherwise EGFP-negative (Fig. 6F,G, white arrows). Presence of EGFP signal in the host hepatocytes is consistent with the idea that the nanotubular structures formed intercellular connections that allow exchange of cell components, although there is at this time no direct data indicating the role of these structures between adjacent engrafted and host cells. Moreover, chMSCs appear to be non-oncogenic, and no visible tumors developed the experimental mice receiving chMSCs.

DISCUSSION

Remarkably, our data showed that chMSCs can transdifferentiate into hepatocytes in response to cues from an injured liver environment by cell fusion independent mechanism. This result is consistent with Kuo et al. [2008], that also showed clonally derived human MSCs engrafted into recipient liver can differentiate into functional hepatocytes. In addition to hepatocyte differentiation, our data strongly suggest the proliferative capacity of chMSC-derived cells in an injured liver microenvironment.

A number of different isolation techniques and culture procedures have been utilized to obtain multipotential MSCs from different sources [Pittenger et al., 1999; Colter et al., 2001; Reyes et al., 2001; Jones et al., 2002; D'Ippolito et al., 2004], and usually, these rare cells have to be maintained in media containing cytokine cocktails [Schwartz et al., 2002; Lee et al., 2004]. Because these MSCs preparations were not clonally purified and remained heterogeneous, the presence of other unknown cell types cannot be discounted. The authentic multipotency of MSCs need to be determined by using clonal MSC lines. In this report, we demonstrate

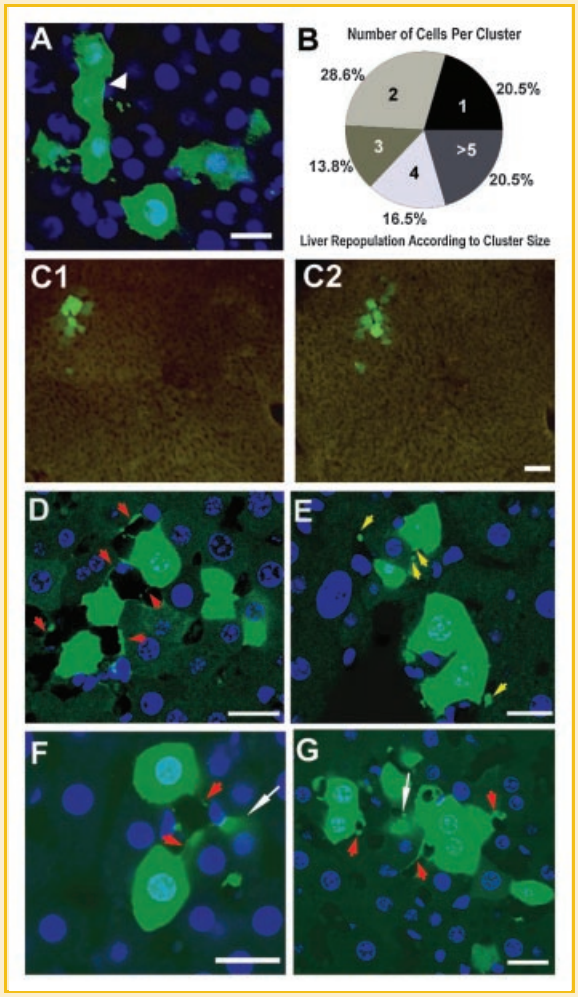

Fig. 7. Engrafted chMSC-derived cells proliferated and formed nanotubular intercellular connections with adjacent host hepatocytes. A is a representative view of a tightly connected cluster of EGFP-positive cells (white arrowhead). B summarizes the distribution of EGFP-positive cells (expressed as % of total EGFP-positive cells) in cell clusters from 1, 2, 3, 4, and >5 cells. C1 and C2 are serial confocal views showing the three-dimensional architecture of the transplanted cell clusters. D–G are representative views showing EGFP-positive nanotubular intercellular connections (red arrowheads) and microvesicles (yellow arrowheads) between EGFP-positive engrafted cells and host hepatocytes. Instances of EGFP expression in the cell membrane and part of the cytoplasm of host hepatocytes are denoted by white arrows. (Scale bar: A, D, E, F, G, 20 μm; C1 and C2, 100 μm.)

that multipotential MSCs are present in the quickly proliferating clonogenic fibroblastic cell fraction of human bone marrow primary cultures. Further, we have clonally isolated lines from these rapidly proliferating fibroblastic cells with all the properties of a multipotential MSCs. These lines, which we term chMSCs, can be maintained in standard medium for classical MSCs [Pittenger et al., 1999]. The multipotency of chMSCs were implicated by the fact that (1) chMSCs express the putative multipotent MSCs marker CD13 [Reyes et al., 2001; Schwartz et al., 2002] and pluripotent stem cell marker *OCT4A* [Richards et al., 2004; Pochampally et al., 2004]; (2) chMSCs could differentiate into the cells of endoderm (hepatocyte-like cells), mesoderm and neuroectoderm (data was not shown) when cultured in the appropriate condition; most importantly, (3) after transplantation into carbon tetrachloride-conditioned SCID mice, chMSCs gave rise to hepatocyte-like cellls in vivo. Interestingly, the *α-SMA* was observed to be expressed in chMSCs (see Fig. 2). *α-SMA* is usually expressed in hepatic stellate cells but not hepatocytes. Thus, the possibility that these chMSCs were derived as a reversion after the cells have first undergone an epithelial differentiation cannot be discounted at this time. The finding that the expression of α-SMA is lower at later passages (Fig. 2B, lane 3) than at earlier passages may support this hypothesis.

It is noteworthy that chMSCs were essentially CD133-negative, since recent studies revealed that CD133-positive cells are capable of self-renewal and differentiation into blood cells, mesenchymal cells, and neural cells [Tondreau et al., 2005; Pozzobon et al., 2009]. CD133 antigen seems to be a marker of more primitive hematopoietic progenitors. However, CD133-negative cells derived from bone marrow are also found in multipotent cells of MSCs [Jones et al., 2002; Vogel et al., 2003; Boyd et al., 2009; Bruno et al., 2009]. The chMSCs isolated by us appear to have been derived from this latter category, since they are CD133-negative (see Fig. 2).

Although hMSCs have attracted considerable clinical interest, there is justifiable concern regarding the risk of tumor growth in recipients. In this study, chMSCs have normal and stable DNA content. In addition, no visible neoplasma was found in all of the recipient SCID mice after transplantation. It appears that chMSCs do not have oncogenic properties.

At present, hepatic failure is a frequent disease, with chronic liver failure ranking fifth among mortality factors, as noted by the World Health Organization [Sukhikh and Shtil', 2002]. Hepatocyte transplantation has long been recognized as a potential treatment for life-threatening liver disease. However, the potential of hepatocyte transplantation remains largely untapped because of the severe shortage of usable primary human hepatocytes. An expandable multipotent human MSCs would be of great value as an alternative cell source for hepatocyte transplantation. Little is known about the mechanism of MSC transdifferentiation into the hepatocytes, particularly within the microenvironment of the injured liver. We observed intercellular nanotubular connections between chMSCs-derived hepatocyte-like cells and murine hepatocytes from the host. Published reports have implicated in cell-to-cell communication by facilitating selective transfer of membrane vesicles and organelles [Rustom et al., 2004; Watkins and Salter, 2005; Gerdes et al., 2007]. Nanotubular structures have been observed between MSCs and cardiomyocytes in co-culture, and that nanotubule-mediated transport of intracellular elements to MSC possibly can determine the direction of their differentiation [Koyanagi et al., 2005; Plotnikov et al., 2008]. Thus, it is tantalizing to speculate that cytoplasmic signaling molecules from host-derived hepatocytes, possibly in conjunction with signals from the microenvironment of injured livers, induced transplanted chMSCs to transdifferentiate into hepatocytes.

ACKNOWLEDGMENTS

We are grateful to Zhang Jun PhD for his technical assistance in FACS analysis. Our thanks should also go to Tang Yin for her help

in confocal microscopy imaging. We also thank Professor Zhu Minhua for his help in providing human liver tissue sections.

REFERENCES

Aurich I, Mueller LP, Aurich H, Luetzkendorf J, Tisljar K, Dollinger MM, Schormann W, Walldorf J, Hengstler JG, Fleig WE, Christ B. 2007. Functional integration of hepatocytes derived from human mesenchymal stem cells into mouse livers. Gut 56:405–415.

Barbash IM, Chouraqui P, Baron J, Feinberg MS, Etzion S, Tessone A, Miller L, Guetta E, Zipori D, Kedes LH, Kloner RA, Leor J. 2003. Systemic delivery of bone marrow-derived mesenchymal stem cells to the infarcted myocardium: feasibility, cell migration, and body distribution. Circulation 108:863–868.

Boyd NL, Robbins KR, Dhara SK, West FD, Stice SL. 2009. Human embryonic stem cell-derived mesoderm-like epithelium transitions to mesenchymal progenitor cells. Tissue Eng Part A [Ahead of print] DOI: 10.1089/ten.tea.2008.0351.

Bruno S, Bussolati B, Grange C, Collino F, Verdun Cantogno L, Herrera MB, Biancone L, Tetta C, Segoloni G, Camussi G. 2009. Isolation and characterization of resident mesenchymal stem cells in human glomeruli. Stem Cells Dev 18:867–880.

Chamberlain J, Yamagami T, Colletti E, Theise ND, Desai J, Frias A, Pixley J, Zanjani ED, Porada CD, Almeida-Porada G. 2007. Efficient generation of human hepatocytes by the intrahepatic delivery of clonal human mesenchymal stem cells in fetal sheep. Hepatology 46:1935–1945.

Coleman WB, McCullough KD, Esch GL, Faris RA, Hixson DC, Smith GJ, Grisham JW. 1997. Evaluation of the differentiation potential of WB-F344 rat liver epithelial stem-like cells in vivo. Differentiation to hepatocytes after transplantation into dipeptidylpeptidase-IV-deficient rat liver. Am J Pathol 151:353–359.

Colter DC, Sekiya I, Prockop DJ. 2001. Identification of a subpopulation of rapidly self-renewing and multipotential adult stem cells in colonies of human marrow stromal cells. Proc Natl Acad Sci USA 98:7841–7845.

Dahlke MH, Popp FC, Larsen S, Schlitt HJ, Rasko JE. 2004. Stem cell therapy of the liver—Fusion or fiction? Liver Transpl 10:471–479.

D'Ippolito G, Diabira S, Howard GA, Menei P, Roos BA, Schiller PC. 2004. Marrow-isolated adult multilineage inducible (MIAMI) cells, a unique population of postnatal young and old human cells with extensive expansion and differentiation potential. J Cell Sci 117:2971–2981.

Dirks C, Miller AD. 2001. Many nonmammalian cells exhibit postentry blocks to transduction by gammaretroviruses pseudotyped with various viral envelopes, including vesicular stomatitis virus G glycoprotein. J Virol 75:6375–6383.

Fang B, Shi M, Liao L, Yang S, Liu Y, Zhao RC. 2004. Systemic infusion of FLK1(+) mesenchymal stem cells ameliorate carbon tetrachloride-induced liver fibrosis in mice. Transplantation 78:83–88.

Gerdes HH, Bukoreshtliev NV, Barroso JF. 2007. Tunneling nanotubes: A new route for the exchange of components between animal cells. FEBS Lett 581:2194–2201.

Gupta S, Chowdhury JR. 2002. Therapeutic potential of hepatocyte transplantation. Semin Cell Dev Biol 13:439–446.

Jiang Y, Vaessen B, Lenvik T, Blackstad M, Reyes M, Verfaillie CM. 2002. Multipotent progenitor cells can be isolated from postnatal murine bone marrow, muscle, and brain. Exp Hematol 30:896–904.

Jiang Y, Jahagirdar BN, Reinhardt RL, Schwartz RE, Keene CD, Ortiz-Gonzalez XR, Reyes M, Lenvik T, Lund T, Blackstad M, Du J, Aldrich S, Lisberg A, Low WC, Largaespada DA, Verfaillie CM. 2002. Pluripotency of mesenchymal stem cells derived from adult marrow. Nature 418:41–49.

Jones EA, Kinsey SE, English A, Jones RA, Straszynski L, Meredith DM, Markham AF, Jack A, Emery P, McGonagle D. 2002. Isolation and characterization of bone marrow multipotential mesenchymal progenitor cells. Arthritis Rheum 46:3349–3360.

Kakinuma S, Tanaka Y, Chinzei R, Watanabe M, Shimizu-Saito K, Hara Y, Teramoto K, Arii S, Sato C, Takase K, Yasumizu T, Teraoka H. 2003. Human umbilical cord blood as a source of transplantable hepatic progenitor cells. Stem Cells 21:217–227.

Kollet O, Shivtiel S, Chen YQ, Suriawinata J, Thung SN, Dabeva MD, Kahn J, Spiegel A, Dar A, Samira S, Goichberg P, Kalinkovich A, Arenzana-Seisdedos F, Nagler A, Hardan I, Revel M, Shafritz DA, Lapidot T. 2003. HGF, SDF-1, and MMP-9 are involved in stress-induced human CD34+ stem cell recruitment to the liver. J Clin Invest 112:160–169.

Koyanagi M, Brandes RP, Haendeler J, Zeiher AM, Dimmeler S. 2005. Cell-to-cell connection of endothelial progenitor cells with cardiac myocytes by nanotubes: A novel mechanism for cell fate changes? Circ Res 96:1039–1041.

Kuo TK, Hung SP, Chuang CH, Chen CT, Shih YR, Fang SC, Yang VW, Lee OK. 2008. Stem cell therapy for liver disease: Parameters governing the success of using bone marrow mesenchymal stem cells. Gastroenterology 134:2111–2121.

Lagasse E, Connors H, Al Dhalimy M, Reitsma M, Dohse M, Osborne L, Wang X, Finegold M, Weissman IL, Grompe M. 2000. Purified hematopoietic stem cells can differentiate into hepatocytes in vivo. Nat Med 6:1229–1234.

Lee KD, Kuo TK, Whang-Peng J, Chung YF, Lin CT, Chou SH, Chen JR, Chen YP, Lee OK. 2004. In vitro hepatic differentiation of human mesenchymal stem cells. Hepatology 40:1275–1284.

Malhi H, Irani AN, Gagandeep S, Gupta S. 2002. Isolation of human progenitor liver epithelial cells with extensive replication capacity and differentiation into mature hepatocytes. J Cell Sci 115:2679–2688.

Munoz-Elias G, Marcus AJ, Coyne TM, Woodbury D, Black IB. 2004. Adult bone marrow stromal cells in the embryonic brain: Engraftment, migration, differentiation, and long-term survival. J Neurosci 24:4585–4595.

Newsome PN, Johannessen I, Boyle S, Dalakas E, McAulay KA, Samuel K, Rae F, Forrester L, Turner ML, Hayes PC, Harrison DJ, Bickmore WA, Plevris JN. 2003. Human cord blood-derived cells can differentiate into hepatocytes in the mouse liver with no evidence of cellular fusion. Gastroenterology 124:1891–1900.

Petersen BE, Bowen WC, Patrene KD, Mars WM, Sullivan AK, Murase N, Boggs SS, Greenberger JS, Goff JP. 1999. Bone marrow as a potential source of hepatic oval cells. Science 284:1168–1170.

Pittenger MF, Mackay AM, Beck SC, Jaiswal RK, Douglas R, Mosca JD, Moorman MA, Simonetti DW, Craig S, Marshak DR. 1999. Multilineage potential of adult human mesenchymal stem cells. Science 284:143–147.

Plotnikov EY, Khryapenkova TG, Vasileva AK, Marey MV, Galkina SI, Isaev NK, Sheval EV, Polyakov VY, Sukhikh GT, Zorov DB. 2008. Cell-to-cell cross-t alk between mesenchymal stem cells and cardiomyocytes in coculture. J Cell Mol Med 12:1622–1631.

Pochampally RR, Smith JR, Ylostalo J, Prockop DJ. 2004. Serum deprivation of human marrow stromal cells (hMSCs) selects for a subpopulation of early progenitor cells with enhanced expression of OCT-4 and other embryonic genes. Blood 103:1647–1652.

Pozzobon M, Piccoli M, Ditadi A, Bollini S, Destro R, André-Schmutz I, Masiero L, Lenzini E, Zanesco L, Petrelli L, Cavazzana-Calvo M, Gazzola MV, De Coppi P. 2009. Mesenchymal stromal cells can be derived from bone marrow CD133(+) cells: Implications for therapy. Stem Cells Dev 18:497–510.

Reyes M, Lund T, Lenvik T, Aguiar D, Koodie L, Verfaillie CM. 2001. Purification and ex vivo expansion of postnatal human marrow mesodermal progenitor cells. Blood 98:2615–2625.

Rhim JA, Sandgren EP, Degen JL, Palmiter RD, Brinster RL. 1994. Replacement of diseased mouse liver by hepatic cell transplantation. Science 263:1149–1152.

Richards M, Tan SP, Tan JH, Chan WK, Bongso A. 2004. The transcriptome profile of human embryonic stem cells as defined by SAGE. Stem Cells 22:51–64.

Rustom A, Saffrich R, Markovic I, Walther P, Gerdes HH. 2004. Nanotubular highways for intercellular organelle transport. Science 303:1007–1010.

Sakaida I, Terai S, Yamamoto N, Aoyama K, Ishikawa T, Nishina H, Okita K. 2004. Transplantation of bone marrow cells reduces CCl4-induced liver fibrosis in mice. Hepatology 40:1304–1311.

Sato Y, Araki H, Kato J, Nakamura K, Kawano Y, Kobune M, Sato T, Miyanishi K, Takayama T, Takahashi M, Takimoto R, Iyama S, Matsunaga T, Ohtani S, Matsuura A, Hamada H, Niitsu Y. 2005. Human mesenchymal stem cells xenografted directly to rat liver are differentiated into human hepatocytes without fusion. Blood 106:756–763.

Schwartz RE, Reyes M, Koodie L, Jiang Y, Blackstad M, Lund T, Lenvik T, Johnson S, Hu WS, Verfaillie CM. 2002. Multipotent adult progenitor cells from bone marrow differentiate into functional hepatocyte-like cells. J Clin Invest 109:1291–1302.

Strick-Marchand H, Morosan S, Charneau P, Kremsdorf D, Weiss MC. 2004. Bipotential mouse embryonic liver stem cell lines contribute to liver regeneration and differentiate as bile ducts and hepatocytes. Proc Natl Acad Sci USA 101:8360–8365.

Sukhikh GT, Shtil' AA. 2002. Transplantation of embryonic hepatocytes. Experimental substantiation of a new approach to the therapy of liver failure. Bull Exp Biol Med 134:519–524.

Suzuki A, Zheng YW, Kaneko S, Onodera M, Fukao K, Nakauchi H, Taniguchi H. 2002. Clonal identification and characterization of self-renewing pluripotent stem cells in the developing liver. J Cell Biol 156:173–184.

Tondreau T, Meuleman N, Delforge A, Dejeneffe M, Leroy R, Massy M, Mortier C, Bron D, Lagneaux L. 2005. Mesenchymal stem cells derived from CD133-positive cells in mobilized peripheral blood and cord blood: Proliferation, Oct4 expression, and plasticity. Stem Cells 23:1105–1112.

Vogel W, Grünebach F, Messam CA, Kanz L, Brugger W, Bühring HJ. 2003. Heterogeneity among human bone marrow-derived mesenchymal stem cells and neural progenitor cells. Haematologica 88:126–133.

von Mach MA, Hengstler JG, Brulport M, Eberhardt M, Schormann W, Hermes M, Prawitt D, Zabel B, Grosche J, Reichenbach A, Muller B, Weilemann LS, Zulewski H. 2004. In vitro cultured islet-derived progenitor cells of human origin express human albumin in severe combined immunodeficiency mouse liver in vivo. Stem Cells 22:1134–1141.

Wang X, Ge S, McNamara G, Hao QL, Crooks GM, Nolta JA. 2003. Albumin-expressing hepatocyte-like cells develop in the livers of immune-deficient mice that received transplants of highly purified human hematopoietic stem cells. Blood 101:4201–4208.

Watkins SC, Salter RD. 2005. Functional connectivity between immune cells mediated by tunneling nanotubules. Immunity 23:309–318.

Yamamoto N, Terai S, Ohata S, Watanabe T, Omori K, Shinoda K, Miyamoto K, Katada T, Sakaida I, Nishina H, Okita K. 2004. A subpopulation of bone marrow cells depleted by a novel antibody, anti-Liv8, is useful for cell therapy to repair damaged liver. Biochem Biophys Res Commun 313:1110–1118.